Available online at www.sciencedirect.com

ScienceDirect

Nuclear Data Sheets 118 (2014) 312–315

Nuclear Data Sheets

www.elsevier.com/locate/nds

Recent Developments of the Liège Intranuclear Cascade Model in View of its Use into High-energy Transport Codes

S. Leray,[1,*] A. Boudard,[1] B. Braunn,[1] J. Cugnon,[2] J.C. David,[1] A. Leprince,[1] and D. Mancusi[1]

[1] *CEA/Saclay, IRFU/SPhN, 91191 Gif-sur-Yvette Cedex, France*
[2] *Liège University, Physics Department B5, Liège, Belgium*

Recent extensions of the Liège Intranuclear Cascade model, INCL, at energies below 100 MeV and for light-ion (up to oxygen) induced reactions are reported. Comparisons with relevant experimental data are shown. The model has been implemented into several high-energy transport codes allowing simulations in a wide domain of applications. Examples of simulations performed for spallation targets with the model implemented into MCNPX and in the domain of medical applications with GEANT4 are presented.

I. INTRODUCTION

The Liège Intranuclear Cascade model, INCL4 [1], has originally been developed to describe spallation reactions, i.e. nucleon-induced collisions in the 100 MeV - 3 GeV energy range. Coupled to the ABLA de-excitation code from GSI [2], INCL4 has been extensively compared with experimental data covering a wide range of reaction channels and continuously improved during the last years. In the benchmark of spallation models organized recently under the auspices of IAEA [3], the combination of the INCL4.5 and ABLA07 [4] versions was found [5] to be one of the models giving the best overall agreement with the experimental data.

A new version, INCL4.6, very similar to INCL4.5 for nucleon-induced reaction above 100 MeV but significantly improved for composite projectiles and energies below 100 MeV, has recently been released [6]. It is now implemented into PHITS [7] and in a version of MCNPX [8], coupled respectively to the GEM and ABLA07 de-excitation models. A version fully re-written in C++, INCL++, extended to light-ion beams up to ^{18}O has also been developed and is included into GEANT4 [9].

II. NEW POTENTIALITIES OF THE MODEL

A. Low-energy Composite-particle Induced Reactions

Although from the origin, the INCL4 model was designed to handle reactions with composite particles up to alpha, little attention had been paid to those up to recently. However, when the model is used in transport codes to simulate for instance a complex spallation target, secondary reactions induced by composite particles generated in primary collisions can occur. Since the data libraries available to the public transport codes do not consider yet reactions induced by complex particles, models are used instead. It is therefore necessary to ensure that they correctly predict at least the gross features of these interactions, although this falls well beyond the alleged theoretical limit of validity of INC models. This is why the treatment of low-energy composite particle induced reactions has been improved in [6].

Let us summarize the main modifications: i) the composite projectile is described as a collection of off-shell nucleons with Fermi motion, ensuring full energy and momentum conservation; ii) geometrical spectators, i.e. nucleons not passing through the target volume, are put on-shell and the energy needed to preserve a correct balance is taken from the participant nucleons; iii) if one nucleon tries to enter the target below the Fermi level, all geometrical participants are assumed to fuse with the target nucleus and produce a compound nucleus, which is subsequently passed over to the de-excitation model; iv) the projectile Coulomb deviation is now explicitly taken into account; v) experimental mass tables are used to ensure correct Q-values for all the reaction channels.

The model is now able to rather well predict helium-induced total reaction cross sections [6]. It also reasonably reproduces the different reaction channels that open with increasing incident energy. This is illustrated in Fig. 1, which shows experimental ^{209}Bi(α,xn) cross sections as a function of the incident particle kinetic energy, from the EXFOR experimental nuclear reaction database [10], compared with the model.

* Corresponding author: sylvie.leray@cea.fr

http://dx.doi.org/10.1016/j.nds.2014.04.067
0090-3752/2014 Published by Elsevier B.V.

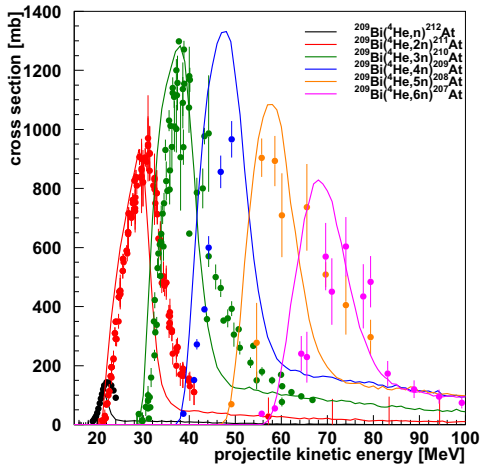

FIG. 1. ^{209}Bi(α,xn) cross sections for x=1 to 6 as functions of the helium kinetic energy compared to the INCL4.6+ABLA07 model. Experimental data come from the experimental nuclear reaction database EXFOR. From [6].

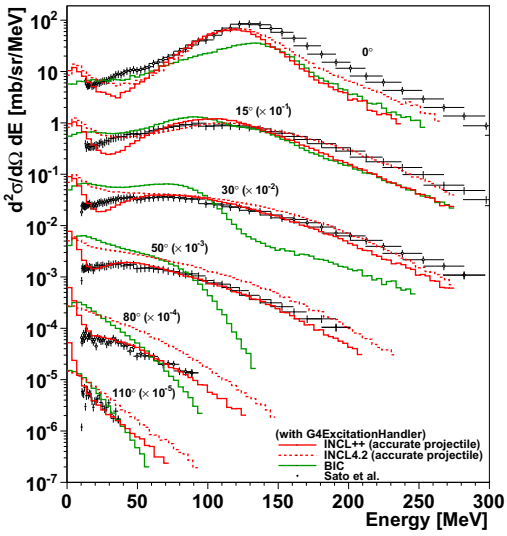

FIG. 2. Neutron production double differential cross sections in the ^{12}C + ^{12}C system at 135 MeV/u [13] compared to INCL++, INCL4.2, both in inverse kinematics, and BIC, all INC coupled to the GEANT4 de-excitation handler.

B. Light-ion Induced Reactions

A first attempt to extend INCL to light-ion induced reactions was done in [11]. Recently, the model has been revisited on the basis of the INCL4.6 version and totally rewritten in C++. This version, denoted as INCL++, has been included in the last GEANT4 release.

In this model, the projectile is described as a collection of nucleons whose positions and momenta are drawn from realistic distributions and satisfy the centre-of-mass constraint of zero total momentum. For each configuration, the depth of a binding potential is determined so that the sum of the nucleon energies is equal to the mass of the projectile nucleus. The projectile is then boosted with the nominal beam velocity. The nucleons that do not interact with this sphere are combined together in the "projectile spectator". The nucleons entering the calculation sphere move globally (with the beam velocity) until one of them interacts with a target nucleon. The NN interaction is then computed with the individual momenta, and Pauli blocking is tested. Nucleons crossing the sphere of calculation without any NN interaction are also combined in the "projectile spectator" at the end of the cascade. A fusion mechanism, as above described is also included.

The excitation energy of the projectile spectator nucleus is obtained by an empirical particle-hole model. This nucleus is then given to the de-excitation model. In this model, this "projectile spectator" has not received any explicit contribution from the zone of interaction which is entirely contained in the target. Therefore, the calculation is not symmetric and the residue of the target is a priori more realistic than the "projectile spectator". This means that to compare with experimental data, if emanating from projectile fragmentation, the results of the calculation should be done in "inverse kinematics" with the target fragments from the calculation Lorentz-boosted to become projectile fragments. Comparisons of ^{12}C+^{12}C experimental data to both "direct" and "inverse kinematics" simulations confirmed that the latter provides a better agreement [12].

Fig. 2 shows neutron production cross-sections measured in the ^{12}C+^{12}C system at 135 MeV by Sato *et al.* [13] compared with the present model, the former version INCL4.2, both in inverse kinematics, and the binary cascade (BIC) [14], all models being coupled to the GEANT4 de-excitation handler [15]. It can be observed that the present model better reproduces the data than the former version and that BIC is definitely less good.

III. EXAMPLES OF APPLICATIONS

A. Radioactive Inventory of the ESS Target

We have used INCL4.6-ABLA07 implemented into MCNPX to simulate the helium-cooled rotating tungsten target foreseen for the ESS facility, in which the radioactive inventory has been determined [16]. The major contributors to the radiotoxicity and their production channel have been identified. In order to estimate the reliability of the simulation, the model has been compared, when possible, with elementary experimental production cross-sections (excitation functions).

Examples of such excitation functions are displayed in Fig. 3 for two nuclides that pose issues for radioprotection: ^{148}Gd, which is an alpha emitter, and tritium. In most of the cases where elementary experimental data are available, the model reproduces them generally within a factor smaller than 2, implying a similar degree of confidence for the estimation of the radioactive inventory.

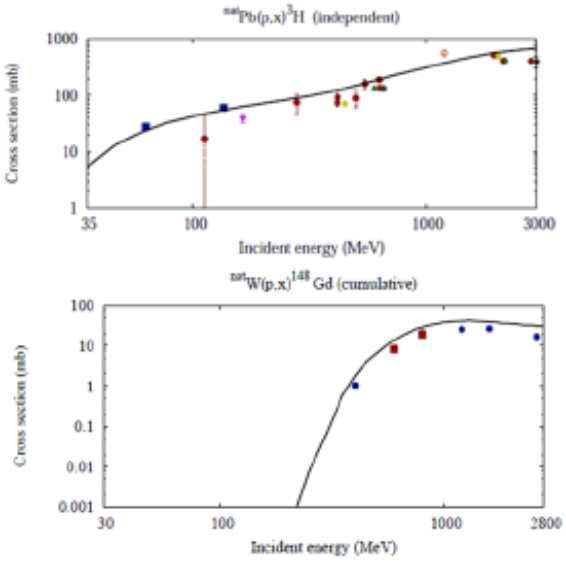

FIG. 3. Experimental production cross sections of ^{148}Gd (lower panel) and tritium (upper panel) in p+W reactions compared with INCL4.6-Abla07. From [16].

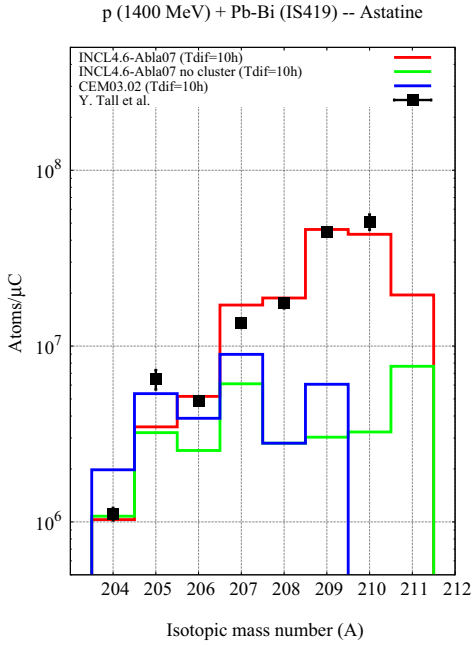

FIG. 4. Astatine release rates from [17] at 1.4 GeV compared to MCNPX simulations, assuming an average release time of 10 hours, with INCL4.6-ABLA07 (red line), INCL4.6-ABLA07 without cluster production by coalescence (green line) and CEM03 (blue line). From [18].

B. Astatine Production in the ISOLDE Target

Recently, the IS419 experiment at the ISOLDE facility at CERN measured the production of astatine isotopes from a liquid lead-bismuth eutectic (LBE) target irradiated by a proton beam of 1 and 1.4 GeV [17]. These isotopes are produced through the following mechanisms: either ^{209}Bi(p,$\pi^- xn$)$^{210-x}$At, i.e. double charge-exchange in primary reactions, or secondary reactions induced by helium nuclei produced in primary collisions, ^{209}Bi(^{3}He,xn)$^{212-x}$At and ^{209}Bi(^{4}He,xn)$^{213-x}$At. The simulation of the ISOLDE experiment with MCNPX [18] has actually revealed that isotopes with mass larger than 209 are produced only through secondary helium-induced reactions, ^4He playing a larger role and leading to higher masses, while the lightest isotopes are populated mostly by double charge-exchange reactions.

Figure 4 shows the result of the MCNPX simulation with INCL4.6-ABLA07 compared to the ISOLDE data at 1.4 GeV for the total production yields of astatine isotopes. An average release time from the liquid metal of 10 hours has been assumed during which the radioactive decay of the different isotopes is taken into account. A remarkable agreement between the calculation and the experiment is observed, regarding not only the shape of the isotopic distribution but also the absolute release rates. Clearly all the new features discussed in the preceding sections, in particular the better handling of low energy helium-induced reactions, have considerably improved the predictive capability of our model compared to the version used in [17].

In order to emphasize the importance of the secondary reactions induced by the clusters produced during the cascade stage through our coalescence mechanism, a calculation has been performed switching off this mechanism. The result is presented as the green curve and exhibits a severe deficit of heavy isotopes. Obviously, a model unable to emit high energy helium nuclei cannot be expected to correctly predict astatine production in a LBE target, since only a small fraction of the heliums produced in the evaporation stage has enough energy to undergo a reaction before being stopped. This is the case of the MCNPX default model option, Bertini-Dresner.

In the same figure, the results are also compared with CEM03 [19] (blue line). It is interesting to note that this model is not able to account for the measured yield of the heavy astatine isotopes. In fact, CEM03 does have mechanisms to produce high-energy helium nuclei; however, helium-induced reactions are handled by the Isabel INC model, which apparently provides an incorrect description in the relevant energy range.

C. Fragmentation of Carbon in PMMA Targets

With the INCL++ model implemented into , it is possible to perform simulations of beam fragmentation experiments in thick targets, which are generally done for hadrontherapy applications. Fig. 5 presents experimental data from Braunn *et al.* [20], concerning nuclear charge distributions from the fragmentation of a 95 MeV/u ^{12}C beam in different thicknesses of PMMA (material mim-

icking the human body) targets, for the 5 *mm* target, at two different angles. The data are compared with our model, BIC and QMD from [21], also available in GEANT4. All models are coupled to the GEANT4 de-excitation.

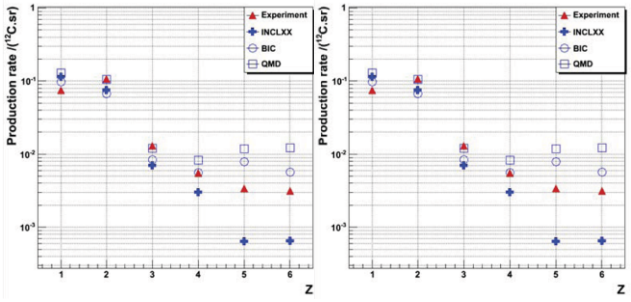

FIG. 5. Charge distribution of fragments produced by a 95 MeV/u ^{12}C beam in a 5 mm PMMA target, at 10° (left) and 20° (right), measured by [20] (red triangles), compared with INCL++ (blue crosses), BIC (blue circles) and QMD (blue squares).

It can be observed that all model reproduce rather well the light ion cross-sections (up to $Z = 4$) but ours tends to underestimates higher charges at 10° while BIC and QMD overestimate these elements. INCL++ and QMD are better at 20°. In general, QMD seems to provide only a slightly better agreement with the data, at the expense of a much longer CPU time.

IV. CONCLUSIONS

We have presented recent extensions of the Liège Intranuclear Cascade model, INCL4, which is now included in several transport codes. They regard first a revisiting of reactions involving low-energy composite particles motivated mainly by the need to correctly account for secondary reactions in spallation targets. Simulations of the ESS and ISOLDE spallation targets were performed. The study on astatine isotopes suggests that our model can be assumed to correctly predict the production of isotopes due to secondary reactions, thanks to the attention paid to the emission of high-energy clusters and to low-energy cluster induced reactions. This is not the case for some of the models widely used in transport codes. Second, the model has been extended to light-ion induced collisions with projectiles up to ^{18}O. Although the treatment of target and projectile is not fully symmetric, but provided that the model is used with the kinematics (direct or inverse) most appropriate to the considered observables, it gives very satisfactory results when compared to different sets of experimental data. Being included in GEANT4, it can be used to simulate thick target problem and gives results generally better than BIC and comparable or only slightly less good than QMD, but with a much shorter CPU time. Further improvements, in particular to make the model for projectile-target symmetrical, and more systematic tests are under progress. A version extended to higher energies has also been developed [22] in which multi-pion channels have been added. Inclusion of strange particle production is also foreseen.

Acknowledgements: This work was partly funded by the FP7 Euratom project ANDES, EC contract number FP7-249671.

[1] A. Boudard *et al.*, Phys. Rev. C **66**, 044615 (2002).
[2] A.R. Junghans *et al.*, Nucl. Phys. A **629**, 635 (1998).
[3] http://www-nds.iaea.org/spallations.
[4] A. Kelic *et al.*, Proc. Joint ICTP-IAEA Advanced Workshop on Model Codes for Spallation Reactions, ICTP Trieste, Italy, February 2008, D. Filges *et al.* Eds., IAEA INDC(NDS)-530, p. 181.
[5] S. Leray *et al.*, J. Korean Physical Soc., **59**, 791 (2011).
[6] A. Boudard *et al.*, Phys. Rev. C **87**, 014606 (2013).
[7] K. Niita *et al.*, JAEA-Data/Code 2010-022 (2010).
[8] J.S. Hendricks *et al.*, Los Alamos National Laboratory Report LA-UR-05-2675 (2005).
[9] S. Agostinelli *et al.*, Nucl. Instrum. Meth. A **506**, 250 (2003).
[10] http://www-nds.iaea.org/exfor/
[11] P. Kaitaniemi *et al.*, Prog. Nucl. Science Tech. **2**, 788 (2011).
[12] S. Leray *et al.*, Proc. 11th Int. Conf. on Nucleus-Nucleus Collisions, San Antonio, USA, May 2012.
[13] H. Sato *et al.*, Phys. Rev. C **64**, 034607 (2001).
[14] G. Folger *et al.*, Eur. Phys. J. A **21**, 407 (2004).
[15] J.M. Quesada *et al.*, Prog. Nucl. Science Tech. **2**, 936 (2011).
[16] A. Leprince *et al.*, Proc. 12th Int. Conf. Radiation Shielding (ICRS-12), September 2012, Nara, Japan.
[17] Y. Tall *et al.*, Proc. Int. Conf. Nuclear Data Science Tech., April 2007, Nice, France, Ed. O. Bersillon *et al.*, EDP Sciences, 1069 (2008).
[18] J.C. David *et al.*, Eur. Phys. J. A **49**, 29 (2013).
[19] S.G. Mashnik *et al.*, J. Phys. Conf. Serv. **41**, 340 (2006).
[20] B. Braunn *et al.*, Nucl. Instrum. Meth. B **269**, 2676 (2011).
[21] T. Koi, Proc. IEEE Nuclear Science Symposium, Dresden, Germany, October 2008.
[22] S. Pedoux and J. Cugnon, Nucl. Phys. A **866**, 16 (2011).